Composite-Fermion Theory for Pseudogap, Fermi Arc, Hole Pocket, and Non-Fermi Liquid of Underdoped Cuprate Superconductors

Youhei Yamaji* and Masatoshi Imada

Department of Applied Physics, University of Tokyo, Hongo, Bunkyo-ku, Tokyo, 113-8656, Japan

(Received 24 May 2010; published 6 January 2011)

We propose that an extension of the exciton concept to doped Mott insulators offers a fruitful insight into challenging issues of the copper oxide superconductors. In our extension, new fermionic excitations called cofermions emerge in conjunction to generalized excitons. The cofermions hybridize with conventional quasiparticles. Then a hybridization gap opens, and is identified as the pseudogap observed in the underdoped cuprates. The resultant Fermi-surface reconstruction naturally explains a number of unusual properties of the underdoped cuprates, such as the Fermi arc and/or pocket formation.

DOI: 10.1103/PhysRevLett.106.016404 PACS numbers: 71.10.Fd, 71.10.Hf, 71.30.+h, 74.72.−h

Since the discovery of cuprate superconductors, the nature of low-energy electronic excitations evolving in their normal metallic phase has attracted much attention as one of the central issues in condensed matter physics. One reason for the interest lies in its connection to the origin of the high temperature superconductivity itself.

Electronic states in the underdoped cuprates are unconventional. For example, spin and charge excitations are unexpectedly suppressed as "pseudogap phenomena" in the normal state. Recent improvement of experimental tools, such as angle-resolved photoemission spectroscopy (ARPES), has further enabled resolving strong momentum dependence of quasiparticles (QPs) [1–3]. In particular, QPs are hardly observed around antinodal points (π, 0) and (0, π) in the 2D Brillouin zone for the CuO_2 plane. It looks like a truncation of a large Fermi surface observed in the overdoped cuprates, and is sometimes called the "Fermi arc." More fundamentally, the normal state of the cuprates remains a challenge as Mott physics in the proximity to the Mott insulator [4]. Although the doped Mott insulators in two dimensions have been studied for a long time using various theoretical approaches [5–17], the nature of the electronic states is not yet fully understood. Recently revealed pseudogap and arc or pocket of the Fermi surface [1–3] require a conceptually deeper understanding for Mott physics.

In this Letter, we elucidate a key role of excitonlike physics on this issue, rather than widely discussed antiferromagnetic [18] and superconducting [19] fluctuations. Excitons are known to be a key concept in physics of semiconductors [20,21]. The excitonic state also emerges in the Mott insulator, for instance as the charge transfer excitation at the optical gap edge in the cuprates [22–24], due to a strong binding of empty (holon) and doubly occupied (doublon) sites in half-filled Mott insulators. In the doped Mott insulators, in spite of screening by doped carriers, the remnant of the binding may still remain as weak binding between a doped holon and the preexisting doublons similarly to excitons. When an electron or hole is added to the doped Mott insulators, it may appear as a normal QP extended in space. However, an electron (a hole) can alternatively be added locally to a holon (doublon) site with a small cost of the on-site Coulomb repulsion. This generates a bound composite particle (cofermion) consisting of the preexisting holon (doublon) and the added electron (hole). We call such cofermions (CFs) *holo-electron* (*doublo-hole*).

A CF (a holo-electron or a doublo-hole) dynamically breaks up into (and recombines from) a conventional QP and a charge boson. This dynamic process is naturally interpreted as a hybridization between the CF and the QP. Here, we show that the resultant hybridization gap offers a natural understanding of a number of key properties of the underdoped cuprates [4] such as Fermi pocket or arc formation [1–3], pseudogap behavior seen in the single particle spectra [2,25], specific heat [26,27], the asymmetric density of states (DOS) [28], and violation of the Wiedemann-Franz law [29,30], without any symmetry breaking. We specifically predict that the pseudogap opens as a *s*-wave-like gap in the *unoccupied* part above the Fermi level contrary to the widely assumed *d*-wave structure.

We study the Hubbard Hamiltonian on a square lattice,

$$\hat{H} = \sum_{i,j} t_{ij} \hat{c}^{\dagger}_{i\sigma} \hat{c}_{j\sigma} + U \sum_{i} \hat{n}_{i\uparrow} \hat{n}_{i\downarrow}, \qquad (1)$$

where $\hat{c}^{\dagger}_{i\sigma}$ ($\hat{c}_{i\sigma}$) is spin-σ creation (annihilation) operator at a site i, while $\hat{n}_{i\sigma} = \hat{c}^{\dagger}_{i\sigma}\hat{c}_{i\sigma}$. For the hopping t_{ij}, we take only $-t$ for the nearest-neighbor and t' for the next-nearest-neighbor pairs.

We first employ the Kotliar-Ruckenstein slave-boson formalism [31], while the local Hilbert space of the Hubbard model is expanded not by the original electron $\hat{c}_\sigma$ but instead by introducing a fermion $\hat{f}_\sigma$, which stands for the σ-spin QP, following Ref. [32] and one slave boson for each Fock state as $\hat{e}$ for the empty state (holon) $|0\rangle$, $\hat{p}_\sigma$ for the singly occupied state $|\sigma\rangle$ ($\sigma =\uparrow$, or $\downarrow$), and $\hat{d}$ for the doubly occupied state (doublon) $|\uparrow\downarrow\rangle$. After the mapping, the Coulomb repulsion U is now interpreted as a "chemical potential" for $\hat{d}_i^\dagger$, while the correlation now appears, as we describe below, in hopping process of $\hat{f}_{i\sigma}^\dagger$ disturbed by slave-boson motion under the local constraints $\hat{e}_i^\dagger \hat{e}_i + \sum_\sigma \hat{p}_{i\sigma}^\dagger \hat{p}_{i\sigma} + \hat{d}_i^\dagger \hat{d}_i = 1$ and $\hat{f}_{i\sigma}^\dagger \hat{f}_{i\sigma} = \hat{p}_{i\sigma}^\dagger \hat{p}_{i\sigma} + \hat{d}_i^\dagger \hat{d}_i$ imposed to keep consistency between the boson and fermion Hilbert space. In the enlarged Hilbert space, these two constraints are assured, respectively, by the Lagrange multipliers $\lambda_i^{(1)}$ and $\lambda_{i\sigma}^{(2)}$ in the Lagrangian as

$$\hat{\mathcal{L}} = \sum_{ij} \hat{f}_{i\sigma}^\dagger(\tau)[\hat{D}_i \delta_{ij} + \hat{\zeta}_{ij\sigma}(\tau) t_{ij}] \hat{f}_{j\sigma}(\tau) + \hat{\mathcal{L}}_B^{(0)}, \quad (2)$$

where $\hat{D}_i = \partial_\tau - \mu + \lambda_{i\sigma}^{(2)}$, $\hat{\zeta}_{ij\sigma}(\tau) = \hat{z}_{i\sigma}(\tau)\hat{z}_{j\sigma}^\dagger(\tau)$, and $\hat{z}_{i\sigma} = \hat{g}_{i\sigma}^{(1)}(\hat{p}_{i\sigma}^\dagger \hat{e}_i + \hat{d}_i^\dagger \hat{p}_{i\bar{\sigma}})\hat{g}_{i\sigma}^{(2)}$ ($\hat{g}_{i\sigma}^{(1)} = (1 - \hat{p}_{i\bar{\sigma}}^\dagger \hat{p}_{i\bar{\sigma}} - \hat{e}_i^\dagger \hat{e}_i)^{-1/2}$ and $\hat{g}_{i\sigma}^{(2)} = (1 - \hat{p}_{i\sigma}^\dagger \hat{p}_{i\sigma} - \hat{d}_i^\dagger \hat{d}_i)^{-1/2}$, following the literature [31]). A part of the Lagrangian $\hat{\mathcal{L}}_B^{(0)}$ contains $\lambda_i^{(1)}$, $\lambda_{i\sigma}^{(2)}$ and quadratic terms of bosonic fields only [31] as, $\hat{\mathcal{L}}_B^{(0)} = \sum_i \{\tilde{e}_i^\dagger(\tau)[\partial_\tau + \lambda_i^{(1)}]\tilde{e}_i(\tau) + \sum_\sigma \tilde{p}_{i\sigma}^\dagger(\tau)[\partial_\tau + \lambda_i^{(1)} - \lambda_{i\sigma}^{(2)}]\tilde{p}_{i\sigma}(\tau) + \tilde{d}_i^\dagger(\tau)[\partial_\tau + U + \lambda_i^{(1)} - \sum_\sigma \lambda_{i\sigma}^{(2)}]\tilde{d}_i(\tau)\}$. To take into account the Gaussian fluctuations of the bosonic fields beyond the mean-field level [33], the Bogoliubov prescription is used, where the boson operators $\hat{b}_i$ ($b = e$, d or p_σ) are divided into condensate $\bar{b}_0$ and fluctuating components $\tilde{b}_i$ as $\hat{b}_i^\dagger = \bar{b}_0 + \tilde{b}_i^\dagger$, $\hat{b}_i = \bar{b}_0 + \tilde{b}_i$.

In this Letter, we make further progress by considering low-energy dynamics arising from coupled bosons and fermions. First, we reexamine the strong coupling ($U/t \to +\infty$) limit [8,17], where adding a σ-spin electron is possible only to $|0\rangle$, namely, a holon site, to avoid creating $|\uparrow\downarrow\rangle$ (doublon) with the cost of U. Creation operators for the electron at $|0\rangle$ are given by $\hat{e}_i \hat{f}_{i\sigma}^\dagger$.

When t/U becomes nonzero, an added electron may become a coherent QP. However, we still have rather localized character of holons, and it allows alternatively forming a collective excitation of a hole and the added electron similarly to an exciton. This collective character is clearly distinguished from the conventional QP. In fact this composite-fermion does not have charge in contrast to the QP [34]. Our crucial step is to include dynamics of this composite fermion expressed by $\tilde{e}_i \hat{f}_{i\sigma}^\dagger$ ($\hat{f}_{i\sigma} \tilde{e}_i^\dagger$).

When we impose the local constraints more strictly for fluctuating bosons beyond the mean-field level, it turns out that, in the hopping process of $\hat{f}_\sigma$ expressed by $\hat{f}_{i\sigma}^\dagger \hat{\zeta}_{ij\sigma} t_{ij} \hat{f}_{j\sigma}$, the coefficient $\hat{\zeta}_{ij\sigma}^{(1)} = g_{1\sigma}^2 g_{2\sigma}^2 (\tilde{p}_{i\sigma}^\dagger \tilde{e}_i + \tilde{d}_i^\dagger \tilde{p}_{i\bar{\sigma}})(\tilde{e}_j^\dagger \tilde{p}_{j\sigma} + \tilde{p}_{j\bar{\sigma}}^\dagger \tilde{d}_j)$ is dominating [35]. Here we employ $g_{1\sigma} = (1 - \bar{p}_{0\bar{\sigma}}^2 - \bar{e}_0^2)^{-1/2}$ and $g_{1\sigma} = (1 - \bar{p}_{0\sigma}^2 - \bar{d}_0^2)^{-1/2}$ following Ref. [31]. This vertex stands for the *backflow* consisting of bosons, due to QP motions.

Then we treat coupling of charge bosons and QPs in $\hat{f}_{i\sigma}^\dagger \hat{\zeta}_{ij\sigma}^{(1)} \hat{f}_{j\sigma}$, which represents a part of the electron-electron interactions in the Hamiltonian (1), by interpreting the form such as $\hat{f}_{i\sigma}^\dagger \tilde{b}_i \tilde{b}_j^\dagger \hat{f}_{j\sigma}$ as the decoupled product of $\hat{\boldsymbol{C}}_{i\sigma}^\dagger = (\tilde{e}_i, \tilde{d}_i^\dagger)\hat{f}_{i\sigma}^\dagger$ and $\hat{\boldsymbol{C}}_{i\sigma} = \hat{f}_{i\sigma}(\tilde{e}_i^\dagger, \tilde{d}_i)^T$. Namely, this boson-QP interaction is equivalently treated by introducing integrals over the Grassmanian Stratonovich-Hubbard fields $\hat{\boldsymbol{\Upsilon}}_{i\sigma}^\dagger = (\hat{\psi}_{i\sigma}^\dagger, \hat{\chi}_{i\sigma}^\dagger)$ as $\hat{\boldsymbol{C}}_{i\sigma}^\dagger \hat{\boldsymbol{C}}_{j\sigma} \to \hat{\boldsymbol{C}}_{i\sigma}^\dagger \hat{\boldsymbol{\Upsilon}}_{j\sigma} + \hat{\boldsymbol{\Upsilon}}_{i\sigma}^\dagger \hat{\boldsymbol{C}}_{j\sigma} - \hat{\boldsymbol{\Upsilon}}_{i\sigma}^\dagger \hat{\boldsymbol{\Upsilon}}_{j\sigma}$.

The newly introduced Grassmann fields $\hat{\psi}_{i\sigma}^\dagger$ and $\hat{\chi}_{i\sigma}^\dagger$ are physically interpreted as CFs, the holo-electron and doublo-hole, respectively. Then, $\hat{\boldsymbol{C}}_{i\sigma}^\dagger \hat{\boldsymbol{\Upsilon}}_{j\sigma} + \hat{\boldsymbol{\Upsilon}}_{i\sigma}^\dagger \hat{\boldsymbol{C}}_{j\sigma}$ is naturally interpreted as breakup and recombination processes of the CFs. After integrating fluctuating bosons out, as mentioned below, it results in the hybridization between CFs $\hat{\psi}_\sigma$, $\hat{\chi}_\sigma$ and QPs $\hat{f}_\sigma$.

We treat Gaussian fluctuations of bosons, and the dynamic coupling between QPs and CFs by using a set of the Dyson equations up to the second order of t_{ij}, as depicted in Fig. 1: Thick lines (thick wavy lines) stand for the dressed Green's functions of the charge bosons $\mathcal{A}^{ab}(r,\tau) = -\langle T\beta_i^a(\tau)\beta_j^{b\dagger}(0)\rangle$ (spin bosons $\mathcal{C}^{ab}(r,\tau) = -\langle T\phi_i^a(\tau)\phi_j^{b\dagger}(0)\rangle$), where a, $b = 1$, 2, $r = i - j$, $(\beta_i^1, \beta_i^2) = (\tilde{e}_i, \tilde{d}_i)$, and $(\phi_i^1, \phi_i^2) = (\tilde{p}_{i\sigma}, \tilde{p}_{i\bar{\sigma}}^\dagger)$. Here we neglect the coupling between charge and spin bosons such as $\langle \tilde{p}_{i\sigma}^\dagger \tilde{e}_i\rangle$, since it becomes small scaled by the doping rate x for $|x| \ll 1$. The correction at higher doping is left for future studies. Thick lines with arrows represent the dressed QPs $\mathcal{G}_\sigma^{(f)}(r,\tau)$. Thin lines [thin wavy lines] represent bare propagators of the charge bosons $\mathcal{A}_0^{ab}(r,\tau)$ [spin bosons $\mathcal{C}_0^{ab}(r,\tau)$], determined by $\hat{\mathcal{L}}_B^{(0)}$. Thin lines with arrows are bare propagators of the QPs $\mathcal{G}_{0\sigma}^{(f)}(r,\tau)$ determined by $\hat{\mathcal{L}}_0 = \sum_{ij} \hat{f}_{i\sigma}^\dagger(\tau)[\hat{D}_i \delta_{ij} + \zeta_{0\sigma} t_{ij}]\hat{f}_{j\sigma}(\tau)$, where $\zeta_{0\sigma} = g_{1\sigma}^2 g_{2\sigma}^2 (\bar{p}_{0\sigma}\bar{e}_0 + \bar{d}_0 \bar{p}_{0\bar{\sigma}})^2$. The Lagrangian $\hat{\mathcal{L}}_0$ is obtained by decoupling the fluctuating bosons from the Lagrangian $\hat{\mathcal{L}} - \hat{\mathcal{L}}_B^{(0)}$ [see Eq. (2)]. Thick (thin) dashed lines with arrows are the cofermion propagators $\mathcal{F}^{cd}$ ($\mathcal{F}_0^{cd} = \delta_{cd}/\epsilon$ with $\epsilon \to 0$) (c, $d = \psi$, χ). This peculiar divergence of $\mathcal{F}_0^{cd}$ is because the Lagrangian does not include CFs if we neglect the interactions between bosons and fermions. By solving the Dyson equations, we obtain the propagators for the QPs and CFs. Here the bosonic

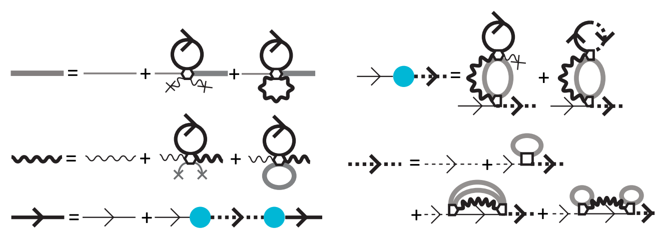

FIG. 1 (color online). Diagrams for the Dyson equations. Solid (dashed) lines with arrows represent propagators of the QPs (CFs). Wavy (solid) lines stand for the charge (spin) bosons. Condensations of bosons are represented by lines terminated at crosses. Coupling constant $g_{1\sigma}^2 g_{2\sigma}^2 t_{ij}$ is represented by open polygons. Here, we do not distinguish holons and doublons. Spins and "flavors" of CFs (ψ, χ) are also not distinguished in the diagram, for simplicity. Filled circles stand for the amplitude of the hybridization between QPs and CFs.

degrees of freedom are taken into account in a self-consistent fashion, through the CF self-energy and the amplitude of hybridization between the QPs and CFs.

Now we show how our self-consistent solution of coupled QPs, bosons and CFs predicts normal-state properties. We show the result at $U = 12t$ and $t' = 0.25t$ to get insight into the cuprate superconductors by restricting to paramagnetic solutions at temperature $T = 0$. First, we give the spectral functions calculated from the electron Green's function $G_\sigma(k, \omega)$ [35]; $A(k, \omega) = -\mathrm{Im}[G_\sigma(k, \omega)]/\pi$. In Fig. 2(a), we show $A(k, \omega)$ for the hole concentration $x = 0.05$. Two main features are found, as confirmed by numerics [36]: the coherent band arising from the QP around the Fermi level and the remnant of the upper (lower) Hubbard band at $\omega > 6t$ ($\omega < -2t$) generated by dynamics of $\tilde{e}$ and $\tilde{d}$ [33,37].

Here, we focus on reconstructions of the Fermi surface. The QP Green's function is given as [35]

$$G_\sigma^{(f)}(k, \omega) \simeq [\omega - \zeta_{0\sigma}\epsilon_k + \mu - \Sigma_f(k, \omega)]^{-1}, \quad (3)$$

where $\Sigma_f = \Delta(k)^2/(\gamma_k \omega - \alpha_k)$ is the QP self-energy arising from the QP-CF hybridization $\Delta(k)$. Here the CF propagator $(\gamma_k \omega - \alpha_k)^{-1}$ is obtained from the expansion around the CF pole. The QPs Green's function has a hybridization gap due to the hybridization with the CFs and $G_\sigma^{(f)}$ shows the divergence of the QP self-energy given by Σ_f at the zero surface [12,14–16] defined by $\gamma_k \omega - \alpha_k = 0$. In our theory, the zero surface splits the band dispersion and generates a distinct s-wave-like gap [as is seen in Fig. 2(b) and supported by recent numerical observation [15,16]].

Topological transitions occur at $x \simeq 0.13$ and $x \simeq 0.18$ [see Figs. 3(a)–3(d)]. Below $x \simeq 0.13$, the reconstructed Fermi surface consists of nontrivial small hole pockets, as a result of the QP-CF hybridization as we see in Fig. 3(a). It is difficult to distinguish the pockets from the arc structure as we see in Fig. 3(a). This is because the zero surface near the outer part partially destroys the QPs. For $0.13 \lesssim x$, large Fermi surfaces appear, instead of Fermi pockets. For $0.13 \lesssim x \lesssim 0.18$, a holelike surface centered at (π, π), and an electronlike one centered at (π, π) coexist [see Fig. 3(b)]. However, the electronlike surface is hardly seen again because of the nearby zero surface.

A gap Δ_{PG} measured from the Fermi level μ emerges near the antinode, corresponding to the pseudogap in the ARPES as we identify in Fig. 3(e). The pseudogap Δ_{PG} is determined by the hybridization gap $\Delta(k)$, basically scaled by a fraction of t, consistently with numerical studies [13]. The doping dependence of Δ_{PG} is given in Fig. 4(a), in agreement with the ARPES for LSCO [2,25].

For $x \lesssim 0.13$, the density of states (DOS) of the electrons $\hat{c}_{k\sigma}$ at the Fermi level, $\rho_F \simeq -\zeta_0 \int d^2kA_f(k, 0)/4\pi^3$, is clearly suppressed, as illustrated in Fig. 4(b). We compare ρ_F with the specific heat coefficient γ measured for LSCO [26,27] by using the conventional relation $\gamma = \pi^2 \rho_F/3$ at $T = 0$. Our γ is consistent with experiments. The ω-dependence of the DOS shows significant asymmetry around $\omega = 0$ in contrast to the DOS for the noninteracting case [35], which naturally explains the asymmetric averaged tunneling spectra observed in the hole-underdoped cuptrates [28] (see Refs. [38,39] for different interpretations).

The present result slightly depends on the choice of the parameters. For instance, Δ_{PG} decreases from the present result by an amount $\sim 0.05t$ at $t'/t = 0.25$ and $U/t = 15$ or $t'/t = 0.15$ and $U/t = 12$, while the qualitative features are robust.

The present CF contributes to the entropy and the thermal conductivity κ in addition to the QP. On the other

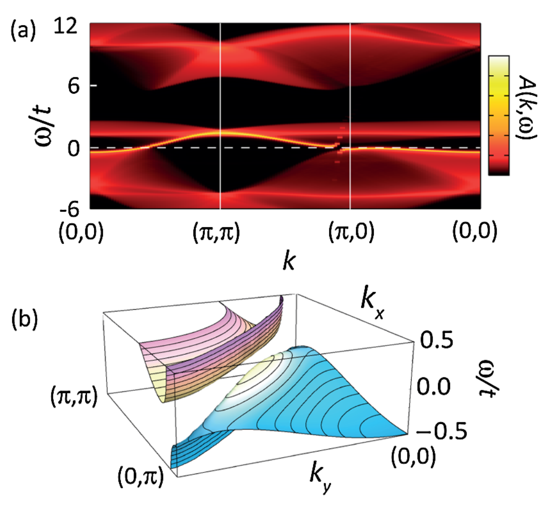

FIG. 2 (color online). Calculated spectral functions for $t'/t = 0.25$, $U/t = 12$ and $x = 0.05$. (a) Spectral function $A(k, \omega)$ along lines running from (0,0), (π,π) and (π,0) to (0,0). The dashed line is the Fermi level. We use a finite broadening factor $\delta = 0.05t$. (b) Band dispersion of QP for $x = 0.05$.

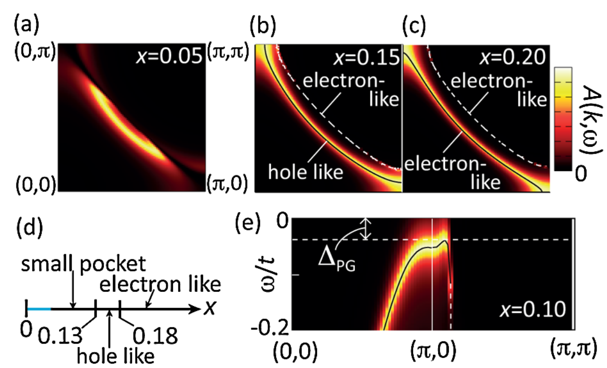

FIG. 3 (color online). Reconstructed Fermi surfaces and spectral functions $A_f(k, \omega)$ for $t'/t = 0.25$ and $U/t = 12$. (a–c) $A_f(k, \omega)(\equiv -\mathrm{Im}[G_\sigma^{(f)}(k, \omega)]/\pi)$ at $\omega = i\delta$. Here we take the broadening factor $\delta = 0.05t$. Solid and dashed lines illustrate the poles of QPs. (d) Doping dependence of Fermi-surface topology in our theory. (e) $A_f(k, \omega)$ along the symmetry line running from (0, 0) through (π, 0) to (π, π) for $x = 0.10$. Thin solid and dashed white lines illustrate poles of QPs. We define Δ_{PG} as the gap between $\mu(\omega = 0)$ and the maximum of the QP dispersion below μ along this symmetry line.

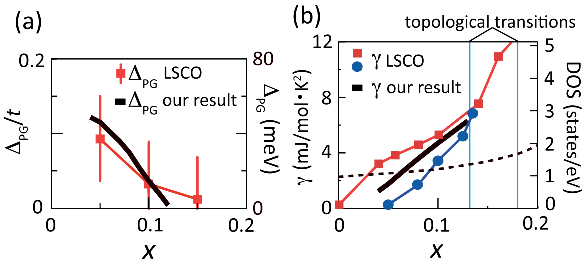

FIG. 4 (color online). (a) Pseudogap Δ_{PG} as a function of hole doping rate x. Thick solid line is Δ_{PG} calculated by our theory. Closed (red) squares show Δ_{PG} estimated from the ARPES [25] for $La_{2-x}Sr_xCuO_4$ (LSCO). (b) DOS of electrons vs x in the present theory (bold solid curve). The thin dashed curve stands for the DOS of the noninteracting case. Closed (blue) circles are obtained by a linear extrapolation of low-temperature normal-state γ of LSCO in Ref. [26] to $T \to 0$, representing the presumable lower limit. Closed (red) squares stand for the estimate for LSCO obtained in Ref. [27] by the Zn doping, which may be an upper limit. All of the present results are obtained at $t = 0.4$ eV, $t'/t = 0.25$ and $U/t = 12$.

hand, the electric conductivity σ is contributed only from the QP. Therefore we expect a serious breakdown of the Wiedeman-Franz law [29,30] that predicts a universal constant $L_0 = \pi^2 k_B^2/3e^2$ for the ratio $L \equiv \kappa/T\sigma$. Our theory predicts $L > L_0$.

We propose to test our specific prediction of the s-wave-like gap structure in unoccupied spectra, for example, by improving the low-energy electron spectroscopies, such as the inverse photoemission, the low-energy electron diffraction spectroscopy, resonant inelastic x-ray spectroscopy, or time resolved photoemission spectroscopy. The midinfrared peak and long tail of the optical conductivity [22] indeed supports our prediction.

Our finding is that hidden cofermionic particles called *holo-electrons* and *doublo-holes* play a key role: The CFs hybridize with the QPs and cause a hybridization gap identified as the pseudogap. A number of resultant properties consistent with the unusual normal states of the cuprates support relevance of our cofermion theory to physics of the cuprates.

The authors thank Yukitoshi Motome and Shiro Sakai for useful discussions. Y. Y. is supported by the Japan Society for the Promotion of Science.

*yamaji@solis.t.u-tokyo.ac.jp

[1] A. Damascelli, Z. Hussain, and Z.-X. Shen, Rev. Mod. Phys. **75**, 473 (2003).
[2] T. Yoshida *et al.*, Phys. Rev. B **74**, 224510 (2006).
[3] J.-Q. Meng *et al.*, Nature (London) **462**, 335 (2009).
[4] M. Imada, A. Fujimori, and Y. Tokura, Rev. Mod. Phys. **70**, 1039 (1998).
[5] J. Hubbard, Proc. R. Soc. A **281**, 401 (1964).
[6] W. F. Brinkman and T. M. Rice, Phys. Rev. B **2**, 4302 (1970).
[7] W. Metzner and D. Vollhardt, Phys. Rev. Lett. **62**, 324 (1989).
[8] M. B. J. Meinders, H. Eskes, and G. A. Sawatzky, Phys. Rev. B **48**, 3916 (1993).
[9] P. A. Lee, N. Nagaosa, and X.-G. Wen, Rev. Mod. Phys. **78**, 17 (2006), and references therein.
[10] E. Dagotto, A. Nazarenko, and M. Boninsegni, Phys. Rev. Lett. **73**, 728 (1994).
[11] N. Furukawa, T. M. Rice, and M. Salmhofer, Phys. Rev. Lett. **81**, 3195 (1998).
[12] I. Dzyaloshinskii, Phys. Rev. B **68**, 085113 (2003).
[13] D. Sénéchal and A.-M. S. Tremblay, Phys. Rev. Lett. **92**, 126401 (2004).
[14] K.-Y. Yang, T. M. Rice, and F.-C. Zhang, Phys. Rev. B **73**, 174501 (2006).
[15] T. D. Stanescu and G. Kotliar, Phys. Rev. B **74**, 125110 (2006).
[16] S. Sakai, Y. Motome, and M. Imada, Phys. Rev. Lett. **102**, 056404 (2009); Phys. Rev. B **82** 134505 (2010) .
[17] P. Phillips, T.-P. Choy, and R. G. Leigh, Rep. Prog. Phys. **72**, 036501 (2009).
[18] J. Schmalian, D. Pines, and B. Stojkovic, Phys. Rev. Lett. **80**, 3839 (1998).
[19] J. R. Engelbrecht *et al.*, Phys. Rev. B **57**, 13 406 (1998); Y. Yanase *et al.*, Phys. Rep. **387**, 1 (2003).
[20] G. D. Mahan, *Many-Particle Physics* (Kluwer Academic/Plenum Publishers, New York, 2000).
[21] B. I. Halperin and T. M. Rice, Rev. Mod. Phys. **40**, 755 (1968).
[22] S. Uchida *et al.*, Phys. Rev. B **43**, 7942 (1991).
[23] D. S. Ellis *et al.*, Phys. Rev. B **77**, 060501 (2008).
[24] R. Schuster *et al.*, Phys. Rev. B **79**, 214517 (2009).
[25] A. Ino *et al.*, Phys. Rev. B **65**, 094504 (2002).
[26] J. W. Loram *et al.*, J. Phys. Chem. Solids **62**, 59 (2001).
[27] N. Momono *et al.*, Physica (Amsterdam) **233C**, 395 (1994).
[28] Ch. Renner *et al.*, Phys. Rev. Lett. **80**, 149 (1998).
[29] R. W. Hill *et al.*, Nature (London) **414**, 711 (2001).
[30] C. Proust *et al.*, Phys. Rev. B **72**, 214511 (2005).
[31] G. Kotliar and A. E. Ruckenstein, Phys. Rev. Lett. **57**, 1362 (1986).
[32] F. Lechermann *et al.*, Phys. Rev. B **76**, 155102 (2007).
[33] C. Castellani *et al.*, Phys. Rev. Lett. **69**, 2009 (1992).
[34] We note the difference of the composite fermion and cofermion, as discussed as follows, from the spinon [9]: Although the cofermion carries a spin but no charge as in the spinon, cofermions coexist with QPs in different part of energy-momentum space in contrast to the spinons.
[35] See supplementary material at http://link.aps.org/supplemental/10.1103/PhysRevLett.106.016404 for further theoretical details on the CFs, QP Green's functions, and the QP density of states.
[36] R. Preuss *et al.*, Phys. Rev. Lett. **79**, 1122 (1997); D. Duffy *et al.*, Phys. Rev. B **56**, 5597 (1997).
[37] R. Raimondi and C. Castellani, Phys. Rev. B **48**, 11453 (1993).
[38] P. W. Anderson and N. P. Ong, J. Phys. Chem. Solids **67**, 1 (2006).
[39] J. Nieminen *et al.*, Phys. Rev. Lett. **102**, 037001 (2009).